RSC Advances

PAPER

View Article Online
View Journal | View Issue

Cite this: *RSC Adv.*, 2018, **8**, 1346

Catalytic reactivity of an iridium complex with a proton responsive N-donor ligand in CO_2 hydrogenation to formate†

Gunniya Hariyanandam Gunasekar, ‡[a] Yeahsel Yoon,‡[a] Il-hyun Baek [b] and Sungho Yoon *[a]

Received 11th November 2017
Accepted 12th December 2017

DOI: 10.1039/c7ra12343d

rsc.li/rsc-advances

Catalytic hydrogenation of CO_2 into formic acid/formate is an attractive conversion in the utilization of CO_2. Although various catalysts with high catalytic efficiency are reported, a very few studies have been carried out to correlate/understand the efficacy and stability of the hydrogenation catalysts, which could be helpful to direct the future design strategy of corresponding catalysts. Herein, a half-sandwich iridium complex containing bibenzimidazole as a proton responsive N-donor ligand, [Cp*Ir(BiBzImH$_2$)Cl]Cl, has been synthesized and fully characterized. The generation of an N^- anion by the deprotonation of a bibenzimidazole group resulted in a significant enhancement of activity. The Ir complex showed about 20 times higher catalytic efficiency in the hydrogenation of CO_2 into formate than that of its bipyridine counterpart [Cp*Ir(Bpy)Cl]Cl. The time dependent catalytic activity studies revealed that the initial excellent activity of [Cp*Ir(BiBzImH$_2$)Cl]Cl was reduced when catalytic cycle proceeds; which was found to be the structural instability of the catalyst caused by steric hindrance between the bibenzimidazole and Cp* ligands.

Introduction

Hydrogenation of greenhouse CO_2 gas into formic acid has been a subject of great interest,[1,2] although it suffers from both thermodynamic and kinetic limitations.[3] The high thermodynamic barrier (eqn (1)), however, can be lowered upon usage of a base (eqn (2)) and/or an aqueous medium (eqn (3)).[3] A relatively high kinetic barrier that exists due to the dissociation of H–H bonds and formation of a C–H bond can be overcome by using a suitable catalyst. Various kinds of catalysts operating in organic solvents and supercritical CO_2 solutions have been studied over the past few decades.[4,5]

	$\Delta G°$ (kJ mol^{-1})	$\Delta H°$ (kJ mol^{-1})	
$CO_{2(g)} + H_{2(g)} \rightarrow HCOOH_{(l)}$	32.9	−31.2	(1)
$CO_{2(g)} + H_{2(g)} + NH_{3(aq)} \rightarrow HCOO_{(aq)}^- + NH_{4(aq)}^+$	−9.5	−84.3	(2)
$CO_{2(aq)} + H_{2(aq)} + NH_{3(aq)} \rightarrow HCOO_{(aq)}^- + NH_{4(aq)}^+$	−35.4	−59.8	(3)

The most remarkable progress in recent years has been the development of bipyridine-based homogeneous catalysts.[6] Particularly, complexes containing hydroxyl functional groups such as [Cp*Ir(DHBP)H$_2$O]$^{2+}$ and [Cp*Ir(DHPT)Cl]$^{2+}$ (DHBP = 4,4′-dihydroxy-2,2′-bipyridine; DHPT = 4,7-dihydroxy-1,10-phenanthroline; Cp* = 1,2,3,4,5-pentamethylcyclopentadiene) showed remarkable catalytic efficiency in aqueous solutions (Scheme 1a).[7] It has been claimed that the high activity of these catalysts was attributed to the strong electron donating property of generated O^- ligand(s).[8]

In order to enhance the above proposed electron donating effect of a ligand, here we designed an imidazole based bidentate 2,2′-bibenzimidazole ligand (BiBzImH$_2$). The presence of six π-electrons in a 5-membered imidazole ring with NH functionality is expected to have a high electron donating property than the simple, unprotonated bipyridine ligand (Scheme 1b). Herein, synthesis, characterization and the catalytic reactivity of an iridium complex containing bibenzimidazole ligand [Cp*Ir(BiBzImH$_2$)Cl]Cl (**1**) is reported for the hydrogenation of CO_2 into formate.

Results and discussion

Synthesis and characterization of 1

Himeda *et al.* introduced various electron donating/withdrawing functional groups on *N*,*N*-bidentate ligated Ir complex and systematically studied their effects in the hydrogenation of CO_2 to formate.[9] An Ir complex containing simple bipyridine (bpy) ligand [Cp*Ir(Bpy)]$^{2+}$ was shown to have an initial turnover frequency (TOF) of 0.3 h^{-1} at relatively milder

[a]*Department of Applied Chemistry, Kookmin University, 77 Jeongneung-ro, Seongbuk-gu, Seoul, 136-702, Republic of Korea. E-mail: yoona@kookmin.ac.kr*

[b]*Korea Institute of Energy Research, 152 Gajeong-ro, Yuseong-gu, Daejeon 305-343, Republic of Korea*

† Electronic supplementary information (ESI) available. CCDC 1419395. For ESI and crystallographic data in CIF or other electronic format see DOI: 10.1039/c7ra12343d

‡ Contributed equally to this work.

temperature (50 °C).[10] This TOF value was further increased to 8.6 h^{-1} when one of the pyridine rings of the bpy ligand was replaced with an electron rich imidazole moiety.[10] A similar but more pronounced enhancement was observed while introducing OH functionality on the pyridine site(s).[11] The TOF value was also improved when both of the pyridine sites were replaced with biimidazole ligand (TOF = 20 h^{-1});[10] the generation of N^- anion by the deprotonation of uncoordinated NH groups of imidazole rings and its strong electron donating character was found to be the origin of this enhancement. This was further confirmed by using *N*-methylated biimidazole ligands, where the activity was decreased drastically.[11] These findings showed that the electron-rich ligands such as imidazole can significantly increase the reactivity of an iridium complex. More evidently, the Ir complex containing electron-donating methyl groups on the imidazole backbone $[Cp^*Ir(4MeBiImH_2)]^{2+}$ ($4MeBiImH_2$: 4,4′,5,5′-tetramethyl-biimidazole) demonstrated a highest TOF (36 h^{-1}) among the tested imidazole ligands.[10] Based on this understanding, we anticipated that the $BiBzImH_2$ ligand which have a relatively rich π electrons than $4MeBiImH_2$ would significantly improve the efficiency of the Ir complex.

$BiBzImH_2$ was prepared through the coupling and elimination reaction between oxamide and *o*-phenylenediamine.[12] Complex **1** was prepared by treating 2 equivalents of $BiBzImH_2$ with a chloroform solution of $[IrCp^*Cl_2]_2$ precursor. Yellow crystals of **1** was obtained in a chloroform/pentane system by the vapour diffusion method. X-ray crystallographic structure of **1** has the monoclinic space group $P2_1/n$ with two chloroform molecules and a chloride counter anion in a unit cell (Fig. 1 and S1†) (the three-dimensional packing structure is shown in a Fig. S2†). The coordination environment of the Ir(III) center was composed of two nitrogen atoms of the $BiBzImH_2$ ligand, Cp* moiety (bound in η^5 fashion) and a chloride anion. One additional Cl^- anion was located in the crystal lattice, balancing the charge state. All atoms in $BiBzImH_2$ are placed approximately on one plane with an Ir–N1 and Ir–N2 respective distances of 2.127 (2) and 2.148 (2) Å. The bond distance of Ir–Cl was 2.3941 (7) Å, which was comparable to that of previously reported $[Cp^*Ir(BiImH_2)Cl]Cl$.[13] The bond distances of N1–H and N2–H were 0.844 and 0.833 Å, respectively. The dihedral angle between $BiBzImH_2$ ligand plane and the plane composed of the iridium atom and the two coordinated nitrogen atoms was 6.32 (19)°. The angle of N1–Ir–Cl and N2–Ir–Cl was 86.85° and 86.45° respectively.

UV-visible spectrum of **1** in chloroform solution showed a broad peak at 337 nm with extinction coefficient of 15 000 cm^{-1} M^{-1} (Fig. S3†); which corresponds to intraligand π–π* transitions.[7b,14] An intensive peak at 281.7 *m*/*z* in the electrospray ionization (ESI) measurement was well matched with the expected $[Cp^*Ir(BiBzImH_2)]^{2+}$ with formula $C_{24}H_{25}IrN_4$ (Fig. S4†). This indicates that **1** maintain its composition in the solution medium. The ^1H NMR spectral data showed that the symmetry of $BiBzImH_2$ was broken while coordination to an iridium ion (Fig. S5 and S6b and c†). In addition, a downfield shift for the $BiBzImH_2$ protons compared to that of bare $BiBzImH_2$ ligand was observed, indicating that metalation shifts the electron density towards the Ir metal center. These results demonstrated that the structure of compound **1** was maintained in a solution also.

Structure of 1 in basic solutions

The hydrogenation of CO_2 is usually proceeds under basic conditions; thus, the actual active form of the catalyst can be different from that of the initial compound. Since pK_{a_1} and pK_{a_2} of $BiBzImH_2$ are 11.0 and >16 respectively, the catalyst is expected to have structure $[Cp^*Ir(BiBzimH)^-Cl]$ (**2**) rather than **1** under the basic hydrogenation conditions (Scheme 2).[15] To understand

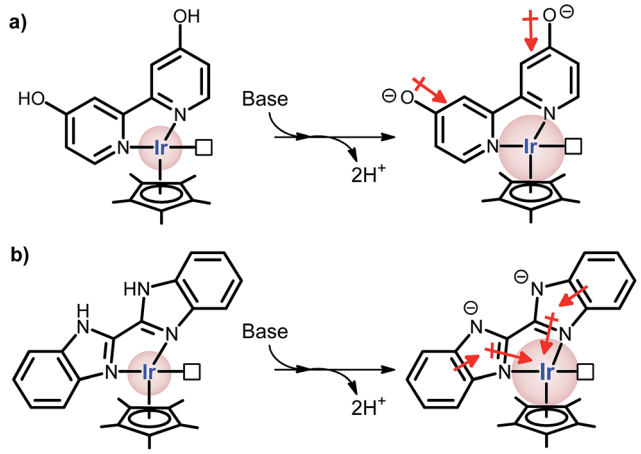

Scheme 1 Representation of expected electron density increment on the Ir centers under basic condition. (a) $[Cp^*Ir(4DHBP)]^{2+}$; (b) $[Cp^*Ir(BiBzImH_2)]^{2+}$.

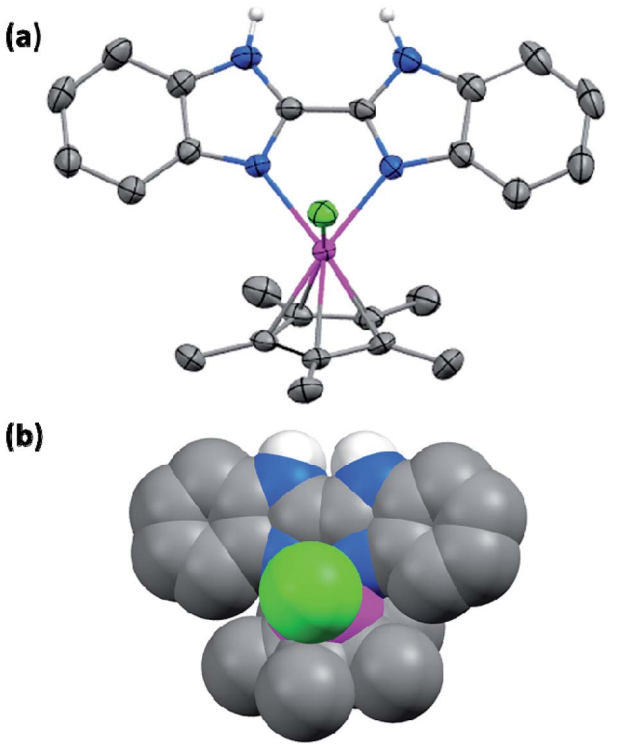

Fig. 1 Crystal structure of **1** (a), with space filling model (b). Solvent molecules, and hydrogen atoms other than NH were omitted for clarity.

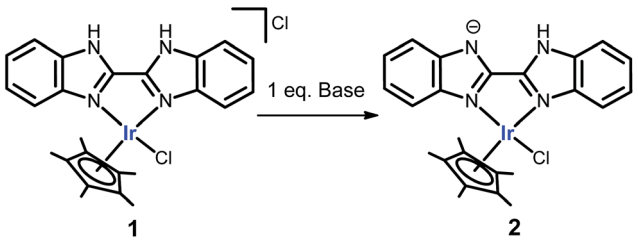

Scheme 2 Deprotonation of **1** in the presence of a base.

this, NMR of **1** with different equivalents of base (triethylamine, Et_3N) was investigated (Fig. 2). In the presence of 1 equivalent of Et_3N, the aromatic protons of **1** were slightly shielded (about 0.1 to 0.18 ppm) and the Cp* protons were slightly deshielded. In addition, it showed a new, broad peak at 3.6 ppm with integral value of 1 (enlarged figure is given in Fig. S6d†). The broad peak can be assigned to a proton held between two nitrogen atoms of $BiBzImH^-$ (Fig. S6d†). A similar change was observed with 4 equivalents of base; importantly, the peak at 3.6 ppm with integral value of 1 does not disappeared. These results indicated that the formation of dianionic (N^{2-}) structure of **1** was difficult, and thus complex **1** may predominantly exists as an N^- ligand (structure **2**) under basic conditions.

Hydrogenation of CO_2

As mentioned above, the hydrogenation of CO_2 is usually performed in aqueous solution, with a base, to overcome the thermodynamic barrier.[3] Because of the limited solubility of **1** in water, however, a mixture of water and methanol (1 : 1) was used in this study. Catalytic activity of **1** was compared with [Cp*Ir(Bpy)Cl]Cl and the results are shown in Table 1. As shown in entry 1, [Cp*Ir(Bpy)Cl]Cl produced a very low formate concentration {[HCO_2^-]} (2.5 mM) in 1 h with a turnover number (TON) of 5. Under similar reaction conditions, the catalyst **1** produced a substantial [HCO_2^-] of 50 mM with TON of 100. This value was 20 times higher than [Cp*Ir(Bpy)Cl]Cl catalyst, confirming that the high electron density of N^- donor ligand results in a higher TON.

In order to gain further insights into the system, time-dependent measurements were performed. As shown in Fig. 3, the rate of formate production was faster at an initial stage of the reaction (TON was 375 in 0.25 h) compared to the final stage of the reaction (TON was 1450 and 1750 in 20 and 38 h, respectively). To clearly visualize this behaviour, the TOF between the hours was plotted *vs.* time (Fig. S7†). It reiterated that the TOF was significantly higher for first 0.25 h (TOF was 1500 h^{-1}) and was decreased rapidly while reaction proceeds (Table S1†).

To understand this, the reaction mixture was analyzed by Mass and NMR spectroscopy after 10 h of hydrogenation. ^1H NMR spectrum showed that the intensity of Cp* peak was remarkably reduced compared to **1**; the ratio between BiBzIm and Cp* was 5 : 1 (Fig. S8†). The ESI-mass measurement showed the presence of various fragments (Fig. S9†). These results suggested that a deformation of the catalyst has occurred during the hydrogenation. Currently we could not find and isolate the decomposed species of **1**, and hence further efforts are needed to investigate the decomposed species and its pathway(s).

One of the major difference between **1** and [Cp*Ir(Bpy)Cl]Cl (in terms of structure) is the use of different N donor ligand. As shown in Table S2,† **1** has longer Ir–N (2.127 Å) and Ir–Cp* (1.789 Å) bond lengths compared to [Cp*Ir(Bpy)Cl]Cl (wherein the values were 2.076 and 1.785 Å, respectively). The electron density mapping of **1** (Fig. 1b) clearly suggests that the observed elongation of Ir–N and Ir–Cp* bond may originate from the steric effect between BiBzIm's benzene ring and the methyl group of Cp*. Since the bond length is inversely proportional to the bond strength, **1** may have weaker bonding interactions, which in turn might led to dissociation. These results shows that the initial excellent activity of catalyst was originated by the strong electron donating property of BiBzIm ligand, and a sharp diminish in activity when the catalytic cycle proceeds was due to its structural instability.

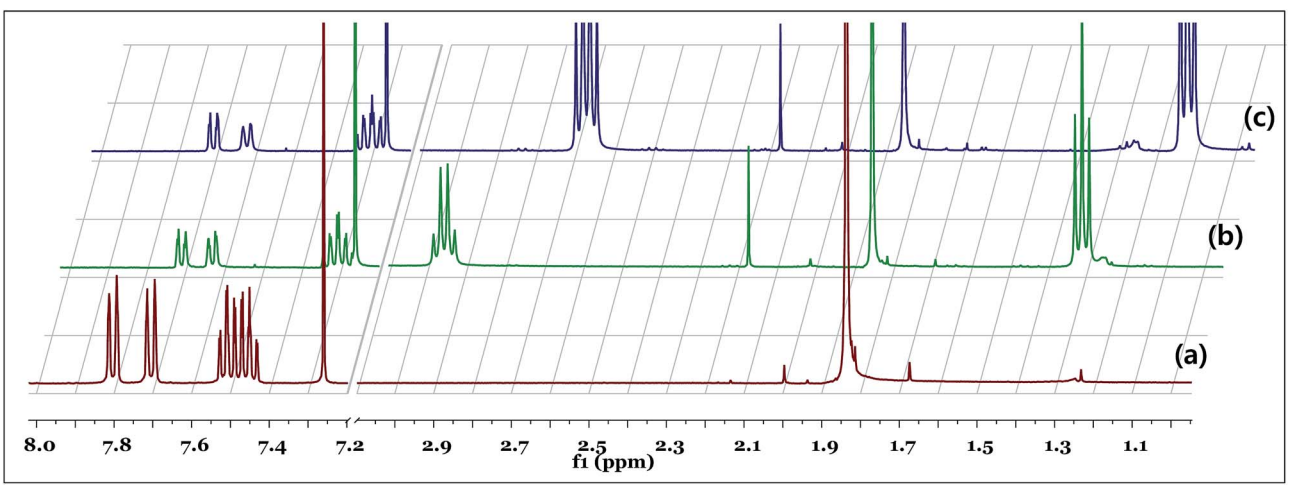

Fig. 2 ^1H NMR of (a) **1**; (b) **1** in the presence of 1 eq. of Et_3N; (c) **1** in the presence of 4 eq. of Et_3N.

Table 1 Hydrogenation of CO_2[a]

Entry	Catalyst	Catalyst conc. (mM)	Time (h)	T (°C)	$[HCO_2^-]$ (mM)	TON[b]
1	[Cp*Ir(Bpy)Cl]Cl	0.5	1	50	2.5	5
2	**1**	0.5	1	50	50	100
3	**1**	0.2	0.25	80	75	375 (1500)[c]
4	**1**	0.2	38	80	350	1750

[a] The reaction was carried out in a 1 M KOH solution of MeOH/H_2O (1 : 1) mixture under 4.0 MPa total pressure ($CO_2/H_2 = 1$). [b] TON = mole of formate/mole of Ir. [c] Initial TOF (h^{-1}); calculated from the initial part of the reaction (after 15 min).

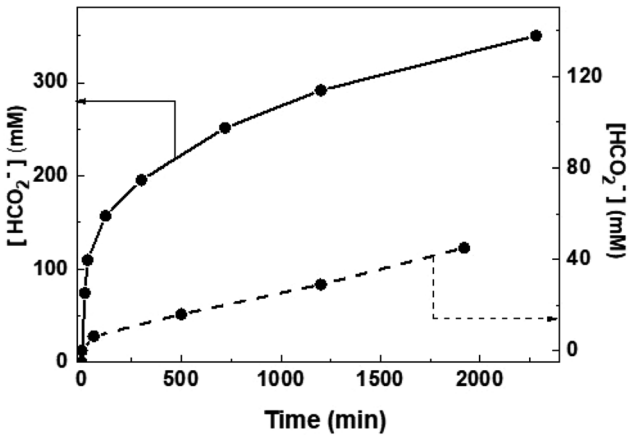

Fig. 3 Time dependent formate generation by **1** (solid line) and [Cp*Ir(Bpy)Cl]Cl (dash line).

Conclusion

In this study, a bibenzimidazole ligated half-sandwich Ir complex [Cp*Ir(BiBzImH_2)Cl]Cl was synthesized and characterized. The Ir complex demonstrated about 20 times higher activity than that of the typical bpy-based catalyst [Cp*Ir(Bpy)Cl]Cl. The generation of N^- anion through the deprotonation of bibenzimidazole NH group is largely responsible for this high catalytic activity. Notwithstanding the forgoing, the activity of Ir complex was dramatically decreased while catalytic cycle proceeds this was found to be the low structural stability of Ir complex under hydrogenation conditions. Previously, it was reported that the decomposition of $[Cp^*Co(Bpy)]^{2+}$ catalyst was attributed to the steric effect caused by the small coordination sphere of cobalt.[16] Iridium-based catalysts are usually known to have a relatively stable structure because of its large coordination sphere and rich coordination sites. Nevertheless, according to this study, in order to achieve a higher efficiency, iridium is required to maintain its stable structural arrangement during the hydrogenation. Thus, stability and electron donating ability are the important factors to be considered while designing the catalysts.

Experimental section

General procedures

All the reagents were purchased from commercial sources and used without further purification unless otherwise described. BiBzImH_2 and $[IrCp^*Cl_2]_2$ were prepared according to literature procedures.[13,17] Electrospray ionization mass spectrometry (ESI-MS) was measured on Agilent 6130 with single quadrupole LC/MS detector. ^{1}H NMR (400 MHz) and ^{13}C NMR (100 MHz) spectra were recorded on a Varian VNMRS500. UV-visible spectra were carried out using S-3100 of SCINCO Co. Ltd.

Synthesis of [Cp*Ir(BiBzImH_2)Cl]Cl (1)

A portion of $[IrCp^*Cl_2]_2$ (0.100 g, 0.126 mmol) was mixed with a chloroform solution (20 mL) of BiBzImH_2 (60.0 mg, 0.256 mmol) under a N_2 atmosphere. After vigorous stirring for 12 h, the insoluble fractions were filtered out and the resulting dark orange filtrate was evaporated to dryness. Yellow crystals of **1** suitable for X-ray diffraction were obtained by vapour diffusion of pentane into the chloroform solution (5 : 2 v/v). Yield: 90.0%. ^{1}H NMR (400 MHz, $CDCl_3$, ppm): δ 14.74 (br s, 2H) 7.81 (dt, J = 7.98, 0.51 Hz, 2H), 7.71 (dt, J = 8.02, 0.74 Hz, 2H), 7.52 (td, J = 7.67, 1.18 Hz, 2H), 7.46 (td, J = 7.70, 1.19 Hz, 2H), 1.84 (*s*, 15H, Cp*); ^{13}C NMR (100.6 MHz, $CDCl_3$, ppm): 144.24, 139.13, 134.35, 126.44, 125.28, 116.65, 115.26, 87.81, 10.44; IR ν/cm^{-1}: 3046(w), 2961(w), 2918(w), 2852(w), 1601(m), 1474(w), 1445(w), 1391(s), 1348(s), 1274(m), 1028(m), 742(s); UV λ_{max} (acetonitrile) 217 (24 675), 267 (4687), 337 (15 046), 356 nm (11 670); ESI-MS (MeOH) (+) (*m*/*z*, relative intensity%): 281.7 (100) $[Cp^*Ir(BiBzImH_2)]^{2+}$, 562.2 (68.3) $[Cp^*Ir(BiBzIm\text{-}H_2)H]^+$.

Note: During the manuscript preparation, Liang *et al.* reported the synthesis of **1** for the methylation of amines.[18]

X-ray crystallographic studies

Single crystal was mounted at room temperature on the tips of quartz fibres, coated with Partone-N oil, and cooled under a stream of cold nitrogen. Intensity data were collected on a Bruker Apex2 diffractometer running the SMART software package, with Mo Kα radiation (λ = 0.71073 Å). The structures were solved by direct methods and refined on F^2 by using the SHELXTL software package.[19] Empirical absorption corrections were applied with SADABS,[20] part of the SHELXTL program package, and the structures were checked for higher symmetry by the program PLATON.[21] All non-hydrogen atoms and amine hydrogens were refined anisotropically. In general, other hydrogen atoms were assigned idealized position and given thermal parameters equivalent to 1.2 times the thermal parameter of the carbon atom to which they are attached. Data collection and experimental details for the complex are summarized in Table S3.†

Hydrogenation activity

Hydrogenation was carried out in a 100 mL homemade stainless steel reactor with glass vessel insert. In a typical run, the complex was added to a water/methanol mixture of KOH solution (50 mL) and saturated the solution with CO_2 for 20 min. The reactor was sequentially pressurized with CO_2 and H_2 (1 : 1) to 40 bar and heated to the desired temperature. The reaction was cooled to room temperature after appropriate time and slowly released the pressure. The concentration of formic acid was analysed by HPLC on an Aminex HPX-87H column with an RI detector using 5.00 mM H_2SO_4 eluent.

Conflicts of interest

There are no conflicts to declare.

Acknowledgements

We acknowledge the financial support by grants from Korea CCS R&D Center, funded by the Ministry of Education, Science and Technology of Korean government. CCDC 1419395† contains the supplementary crystallographic data for this paper.

References

1 (*a*) P. G. Jessop, F. Joo and C. C. Tai, *Coord. Chem. Rev.*, 2004, **248**, 2425–2442; (*b*) P. G. Jessop, Y. Hsiao, T. Ikariya and R. Noyori, *J. Am. Chem. Soc.*, 1996, **118**, 344–355; (*c*) G. Gunniya Hariyanandam, D. Hyun, P. Natarajan, K. D. Jung and S. Yoon, *Catal. Today*, 2016, **265**, 52–55; (*d*) E. Fujita, J. T. Muckerman and Y. Himeda, *Biochim. Biophys. Acta*, 2013, **1827**, 1031–1038; (*e*) G. H. Gunasekar, K. Park, V. Ganesan, K. Lee, N. K. Kim, K. D. Jung and S. Yoon, *Chem. Mater.*, 2017, **29**, 6740–6748.

2 (*a*) C. Federsel, A. Boddien, R. Jackstell, R. Jennerjahn, P. J. Dyson, R. Scopelliti, G. Laurenczy and M. Beller, *Angew. Chem.*, 2010, **49**, 9777–9780; (*b*) K. Park, G. H. Gunasekar, N. Prakash, K. D. Jung and S. Yoon, *ChemSusChem*, 2015, **8**, 3410–3413; (*c*) C. Federsel, R. Jackstell, A. Boddien, G. Laurenczy and M. Beller, *ChemSusChem*, 2009, **3**, 1048–1050; (*d*) A. V. Bavykina, E. Rozhko, M. G. Goesten, T. Wezendonk, B. Seoane, F. Kapteijn, M. Makkee and J. Gascon, *ChemCatChem*, 2016, **8**, 2217–2221; (*e*) J. Jiang, G. H. Gunasekar, S. Park, S. H. Kim, S. Yoon and L. Piao, *Mater. Res. Bull.*, 2018, **100**, 184–190.

3 (*a*) P. G. Jessop, T. Ikariya and R. Noyori, *Chem. Rev.*, 1995, **95**, 259–272; (*b*) G. H. Gunasekar, K. Park, K. D. Jung and S. Yoon, *Inorg. Chem. Front.*, 2016, **3**, 882–895.

4 (*a*) Y. Inoue, Y. Sasaki and H. Hashimoto, *J. Chem. Soc., Chem. Commun.*, 1975, 718–719; (*b*) Y. Inoue, H. Izumida, Y. Sasaki and H. Hashimoto, *Chem. Lett.*, 1976, 863–864.

5 (*a*) P. G. Jessop, T. Ikariya and R. Noyori, *Nature*, 1994, **368**, 231–233; (*b*) P. Munshi, A. D. Main, J. C. Linehan, C.-C. Tai and P. G. Jessop, *J. Am. Chem. Soc.*, 2002, **124**, 7963–7971; (*c*) G. A. Filonenko, R. van Putten, E. N. Schulpen, E. J. M. Hensen and E. A. Pidko, *ChemCatChem*, 2014, **6**, 1526–1530.

6 (*a*) W.-H. Wang, Y. Himeda, J. T. Muckerman, G. F. Manbeck and E. Fujita, *Chem. Rev.*, 2015, **115**, 12936–12973; (*b*) Y. Himeda, *Eur. J. Inorg. Chem.*, 2007, 3927–3941.

7 (*a*) Y. Himeda, N. Onozawa-Komatsuzaki, H. Sugihara and K. Kasuga, *Organometallics*, 2007, **26**, 702–712; (*b*) Y. Himeda, N. Onozawa-Komatsuzaki, H. Sugihara and K. Kasuga, *J. Photochem. Photobiol., A*, 2006, **182**, 306–309.

8 (*a*) W.-H. Wang, J. F. Hull, J. T. Muckerman, E. Fujita and Y. Himeda, *Energy Environ. Sci.*, 2012, **5**, 7923–7926; (*b*) Y. Suna, M. Z. Ertem, W.-H. Wang, H. Kambayashi, Y. Manaka, J. T. Muckerman, E. Fujita and Y. Himeda, *Organometallics*, 2014, **33**, 6519–6530.

9 (*a*) N. Onishi, S. Xu, Y. Manaka, Y. Suna, W.-H. Wang, J. T. Muckerman, E. Fujita and Y. Himeda, *Inorg. Chem.*, 2015, **54**, 5114–5123; (*b*) L. Wang, N. Onishi, K. Murata, T. Hirose, J. T. Muckerman, E. Fujita and Y. Himeda, *ChemSusChem*, 2017, **10**, 1071–1075.

10 Y. Manaka, W.-H. Wang, Y. Suna, H. Kambayashi, J. T. Muckerman, E. Fujita and Y. Himeda, *Catal. Sci. Technol.*, 2014, **4**, 34–37.

11 Y. Suna, Y. Himeda, E. Fujita, J. T. Muckerman and M. Z. Ertem, *ChemSusChem*, 2017, **10**, 4535–4543.

12 B. F. Fieselmann, D. N. Hendrickson and G. D. Stucky, *Inorg. Chem.*, 1978, **17**, 2078–2084.

13 R. Ziessel, *J. Organomet. Chem.*, 1992, **441**, 143–154.

14 M. Kalidasan, R. Nagarajaprakash, S. Forbes, Y. Mozharivskyj and K. M. Rao, *Z. Anorg. Allg. Chem.*, 2015, **641**, 715–723.

15 A. Kumar, H. K. Sinha and S. K. Dogra, *Can. J. Chem.*, 1989, **67**, 1200.

16 Y. M. Badiei, W.-H. Wang, J. F. Hull, D. J. Szalda, J. T. Muckerman, Y. Himeda and E. Fujita, *Inorg. Chem.*, 2013, **52**, 12576–12586.

17 C. White, A. Yates and P. M. Maltlis, *Inorg. Synth.*, 1992, **29**, 228–234.

18 R. Liang, S. Li, R. Wang, L. Lu and F. Li, *Org. Lett.*, 2017, **19**, 5790–5793.

19 *SMART Version 5.618: Bruker Advanced X-ray Solution*, Madison Inc., WI, 2002; *SAINT, Version 6.45: Bruker Advanced X-ray Solution*, Madison Inc., WI, 2003.

20 G. M. Sheldrick, *SHELXTL, Version 6.14: Bruker Advanced X-ray Solution*, Madison Inc., WI, 2003.

21 G. M. Sheldrick, *SADABS, Area-Detector Absorption Correction*, University of Göttingen, Göttingen, Germany, 2001.

